SUBMERGED TURBULENT TWIN JETS INTERACTING WITH A FREE SURFACE AND A SOLID WALL

Ebenezer E. Essel
Department of Mechanical Engineering
University of Manitoba
Winnipeg, MB, Canada, R3T 5V6
essele@myumanitoba.ca

Diya Cui
Department of Mechanical Engineering
University of Manitoba
Winnipeg, MB, Canada, R3T 5V6
cuid345@myumanitoba.ca

Mark F. Tachie
Department of Mechanical Engineering
University of Manitoba
Winnipeg, MB, Canada, R3T 5V6
mark.tachie@umanitoba.ca

ABSTRACT

This paper investigates the effects of offset ratio on the turbulence characteristics of submerged twin jets interacting with a free surface and a solid wall. Experiments were conducted with a particle image velocimetry system at Reynolds number of 5000 for twin jets of separation ratio, $G/d = 2$, where d is the nozzle diameter. The jet adjacent to each boundary was positioned at three offset heights ($1d$, $2d$ and $4d$) from the boundary. The results showed that the effects of confinement constrained the outward growth of the jet closer the boundary, and delayed the combined point as offset height decreased. The interaction with the solid wall increased the reattachment length, the combined point and turbulence intensities compared their free surface counterparts. The size of the large scale structures embodied in the two-point autocorrelations was reduced at lower offset heights.

INTRODUCTION

The interaction of submerged turbulent jets with a boundary is of great interest in geophysical and engineering applications such as pollutant transport in shallow water bodies, pump-jets of ships and air-aerators of water reservoirs. The jet-boundary interaction is influenced by several parameters including Reynolds number, offset ratio and boundary type (free surface or solid wall). For a free surface, kinematic effects prevail at the surface while for a solid wall both viscous and kinematic effects are present at the wall. To improve the fundamental understanding of jet-boundary interaction and the predictive capability of engineering models, there is a need to thoroughly investigate the turbulence characteristics of submerged jets interacting with a free surface and a solid wall.

The physics of turbulence-boundary interaction has been investigated over a long period using flows such as surface jets (Walker et al. 1995), wall offset jets (Agelin-Chaab and Tachie 2011) and turbulent boundary layers (Perot and Moin 1995). Perot and Moin (1995) investigated the effects of free surface and a solid wall on the turbulence statistics using DNS. For both boundary conditions, intercomponent energy transfer between the velocity fluctuations occurred near the boundary. It was argued that the intercomponent energy transfer is due to an imbalance between fluid moving towards the surface in a sweep event (splat) and fluid moving away from the boundary in an ejection event (anti-splat). Walker et al. (1995) carried out experiments to investigate the interaction between a surface round jet and a free surface. They attributed the intercomponent energy transfer near the free surface to vorticity-free surface interaction. The effects of confinement by a solid wall on the turbulence characteristics of an offset jet were investigated by Agelin-Chaab and Tachie (2011). The reattachment length and mean velocity decay reduced as offset height decreased.

Most of the work on jet-boundary interaction were conducted with a single jet (Agelin-Chaab and Tachie 2011; Walker et al. 1995) while the few studies on twin jets focussed on the influence of a solid wall (Wang and Tan 2007). Wang and Tan (2007) examined the interaction between an offset jet and a parallel wall jet and observed that the levels of the Reynolds stresses were enhanced in regions near the wall and the center plane of the jets.

In the present study, a PIV technique is used to investigate the effects of a free surface and a solid wall on the turbulence statistics of submerged twin jets produced from two parallel round nozzles at offset height, $1d$, $2d$ and $4d$ (where d is the nozzle diameter) from each boundary.

EXPERIMENTAL PROCEDURE

The experiments were conducted in a clean open water channel of dimensions 2500 mm long, 200 mm wide and 250 mm deep. The channel walls were made from transparent acrylic plate to facilitate optical access. The submerged twin jets were produced from two round nozzles each of exit diameter, $d = 10$ mm and separation ratio, $G/d = 2$. Figure 1a and 1b show the schematic of the vertical symmetry plane of the twin jets used to investigate the effects of the free surface (STJ-FS) and the solid wall (STJ-SW), respectively. As indicated in each figure, the Cartesian coordinate system has the x-axis aligned with the streamwise direction ($x = 0$ at the exit plane) and y-axis aligned with the transverse direction ($y = 0$ at the center plane of the twin jets). The centerline of the upper jet is at a depth (h) from the free surface while that of the lower jet is at a distance (w) from the bottom wall. For clarity, the jet adjacent to each boundary is denoted as Jet A (JA) and the jet positioned far from the boundary is denoted as Jet B (JB). Experiments were conducted at three offset height ratios for each boundary condition; $h/d = 1$, 2 and 4 for STJ-FS and $w/d = 1$, 2 and 4 for STJ-SW. For each experiment, Jet B was about $14d$ from the free surface or solid wall, and its dynamics was not influenced by the boundary within the measurement span, $45d$ considered herein.

The jet exit velocity and Reynolds number based on the exit velocity and nozzle diameter were kept constant at $U_j = 0.50$ m/s and $Re = 5000$ in each experiment. A PIV system was used to conduct detailed velocity measurements in the channel. The flow was seeded with 10 μm silver coated hollow glass spheres and illuminated with a Nd:YAG double-pulsed laser (120 mJ/pulse). A 12-bit CCD camera was used to image scattered light from the tracer particles. The field of view was set to 120 mm × 120 mm and measurements were acquired in 4 planes extending $45d$ from the exit plane. Based on preliminary convergence test, 10000 image pairs were acquired in each measurement plane to calculate the ensemble statistics. The data was post processed using adaptive correlation algorithm and moving average validation options of DynamicStudio v4.1. The interrogation area size was set to 32 pixels × 32 pixels with 50% overlap in the x-y directions and the resulting spacing between adjacent velocity vectors was $0.094d$.

RESULTS AND DISCUSSION

In this paper, results for the two extreme offset ratios for each boundary condition ($h/d = 1$ and 4, and $w/d = 1$ and 4) are used to examine the effects of the boundary condition and offset ratio on the turbulence statistics of the submerged twin jets.

Mean velocity and Reynolds stresses

Iso-contours of the streamwise mean velocity for $h/d = 1$ and 4 and $w/d = 1$ and 4 are shown in Figure 2. The vector profiles are superimposed on the iso-contours to illustrate the evolution of the submerged twin jets and examine the effects of confinement on the salient features. For each test case, Jet A is deflected towards the boundary and eventually interacts with the boundary beyond the attachment point, L_r. For $h/d = 1$ and $w/d = 1$, the jet-boundary interaction begins in the potential core region ($x/d \leq 3$) while for the higher offset ratios, the interaction occurs in the transition/merging region. For the free surface cases, the interaction between the vortical structures in the jet with the surface increased the surface velocity beyond the attachment point, and the effect is more severe for the lower offset ratio. In the case of the solid wall, a boundary layer developed after reattachment due to the no-slip condition at the wall. These plots indicate that one of the effects of confinement is to limit the outward spread of Jet A compared to Jet B as offset ratio decreased. In the near field, the inner shear layers of the jets deflect towards each other to form a converging region. The deflection of the inner shear layers is caused by a low pressure zone generated between the shear layers due to the mutual entrainment of the fluid between the jets. Similar to 3D twin jets (Harima et al. 2001), the present converging region has no distinct reverse flow. The shape of the vector profiles changes progressively as the vectors near the center plane increase downstream. This behaviour depicts the jet-jet interaction which subsequently leads to the transition of the twin jets to a single combined jet.

The attachment length can be used to characterize the effects of confinement on the submerged jets. Here, the attachment length for the surface-attaching jet is defined
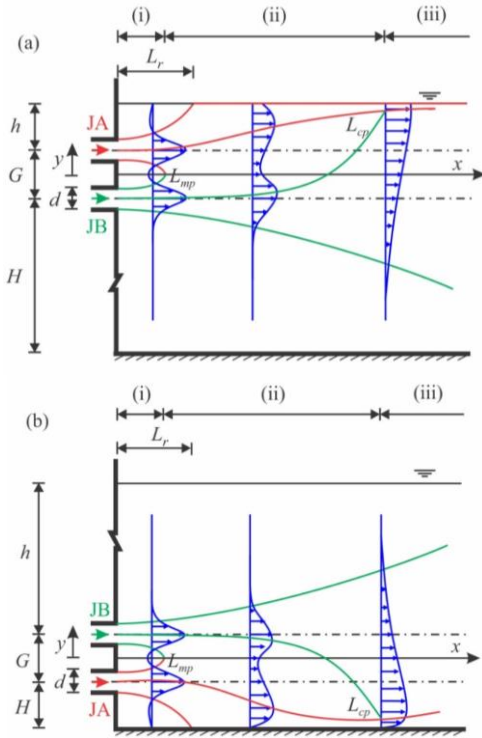

Figure 1. Schematic drawing of submerged twin jets interacting with a free surface, STJ-FS (a) and a solid wall, STJ-SW (b). (i) Converging region (ii) merging region and (iii) combined region.
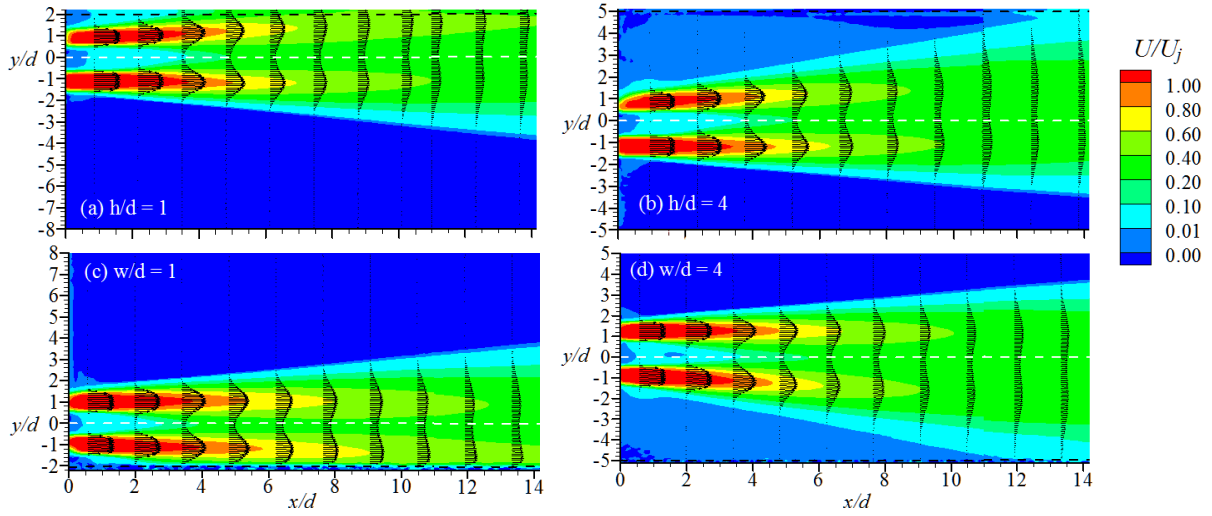
Figure 2. Iso-contours of normalised streamwise mean velocity. Vector profiles are superimposed on the isocontours

as the streamwise location from the exit plane to where the surface velocity is different from zero. For the wall-attaching jet, the attachment point is identified as the location where the $0.01U_j$ contour line attaches onto the wall. This method is used because of the lack of reverse flow in the confined region. The attachment lengths are L_r/d = 0.8, 3.8 and 11.5 for h/d = 1, 2 and 4 and L_r/d = 0.9, 4.7 and 12.1 for w/d = 1, 2 and 4, respectively. The present reattachment lengths are compared to previous surface-attaching twin jets (Essel and Tachie 2017), surface jet (Tay et al. 2017) and wall-attaching single jet (Agelin-Chaab and Tachie 2011) in Figure 3. Except for the data for w/d = 4 from Agelin-Chaab and Tachie (2011), the variation of reattachment length with offset ratio for the present and previous studies can be described by the linear fit:

$$L_r/d = 3.6(h^*/d) - 2.7 \qquad (1)$$

The influence of offset ratio and boundary condition on the mixing characteristics of the submerged twin jets is examined in Figure 4. Figure 4a shows the decay of the

local maximum mean velocity, U_m of Jet A. The plot indicates two stages of velocity decay for each test condition. The first stage is attributed to the initial evolution of the jet which is similar to a free jet. In the second stage, the decay rate is reduced because of confinement effects. The streamwise location where the transition occurs is shorter for the smaller offset ratios (x/d = 10) than the larger offset ratios (x/d = 26), in agreement with the distribution of the reattachment length. A linear fit to the data for x/d > 5 show a decay rate, k_u = 0.220 in the first stage for larger offset ratios. The value of k_u is 0.084 in the second stage for each test case. The decay rate in the first stage agrees with 0.211 reported for free round jet at Re = 5400 (Todde et al. 2009). The distributions of the normalised local mean velocity on the center plane (y = 0), U_c/U_j are
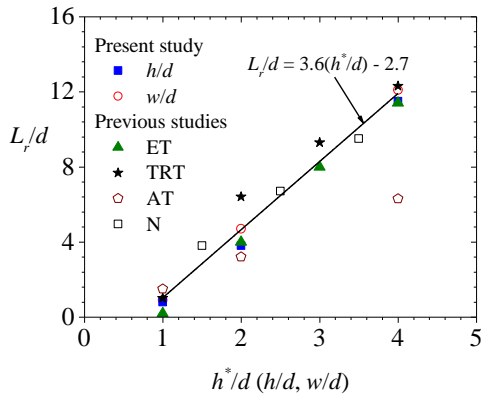

Figure 3. Variation of reattachment length and offset ratio. ET- Essel and Tachie 2017, TRT-Tay et al. 2016, AT- Agelin-Chaab and Tachie (2011), N – Nazoki (1983)
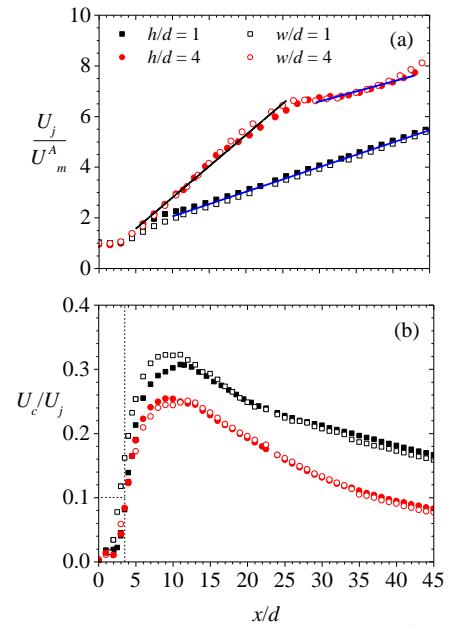

Figure 4. Distribution of maximum mean velocity decay of Jet A (a) and center plane velocity (b)

3
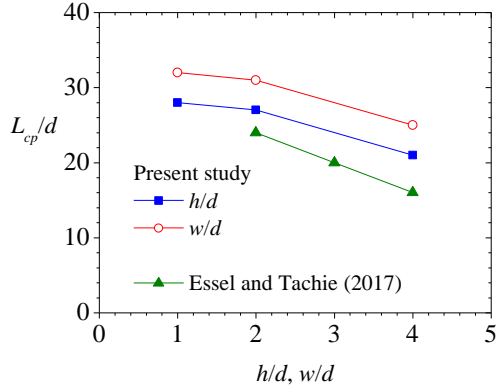
Figure 5. Variation of combined point distance and offset ratio for submerged twin jets.

Figure 6. Profiles of streamwise mean velocity (a), streamwise (b) and transverse (c) Reynolds normal stresses. Where U_m^B is the local maximum mean velocity of Jet B.

shown in Figure 4a. The plot is used to estimate the merging point distance, L_{mp} which is defined as the streamwise distance from the exit plane to the location where the local mean velocity is 10% of the maximum velocity in the flow field. As indicated by the dashed lines, L_{mp} is approximately $3.5d$ for all test cases. The increase in U_c/U_j beyond the merging point is an artifact of the interaction between the inner layers. The higher U_c/U_j profiles for the lowest offset ratios is attributed to the reduced entrainment and mixing as offset ratio decreased.

For free 3D twin jets (Harima et al. 2001), the combined point is defined as the streamwise location from the exit plane where $U_c/U_m = 1$. This definition is not applicable for the submerged twin jets because of the asymmetry imposed by the boundary. Therefore, the combined point is determined as the streamwise location where the point of inflection near the center plane disappears from the streamwise mean velocity profile. The combined point distance, L_{cp}/d for the present study and data from Essel and Tachie (2017) are shown in Figure 5. The plots indicate that the transition of the twin jets to a single jet is delayed as offset ratio decreases and the effects are higher over a solid wall than a free surface. The disparity between the present surface-attaching jets and Essel and Tachie (2017) is likely due to the sensitivity of the combined point to geometric and initial conditions.

Profiles of the normalised streamwise mean velocity and Reynolds normal stresses for $h/d = 4$ and $w/d = 4$ are shown in Figure 6 to examine the effects of the boundary condition on the flow characteristics in the interaction region. The profiles were obtained at $x^*/d = 0$, 10, 20 and 30, where x^* has an origin at the attachment point. In the plots, the y-axis for solid wall profiles is negated to facilitate comparison with the free surface data. The evolution of the mean velocity profiles demonstrates the transition of the twin jets to a wall jet for $w/d = 4$ and a surface jet for $h/d = 4$. The profiles of streamwise and transverse Reynolds normal stresses are presented in Figure 6(b) and (c), respectively. For the streamwise Reynolds normal stress, the peak that develops near each boundary is associated with the reduced transverse Reynolds normal stress near the boundary. This phenomenon is as a result of the intercomponent energy transfer from the transverse Reynolds normal stress to the tangential Reynolds normal stresses due to the vorticity-boundary interaction
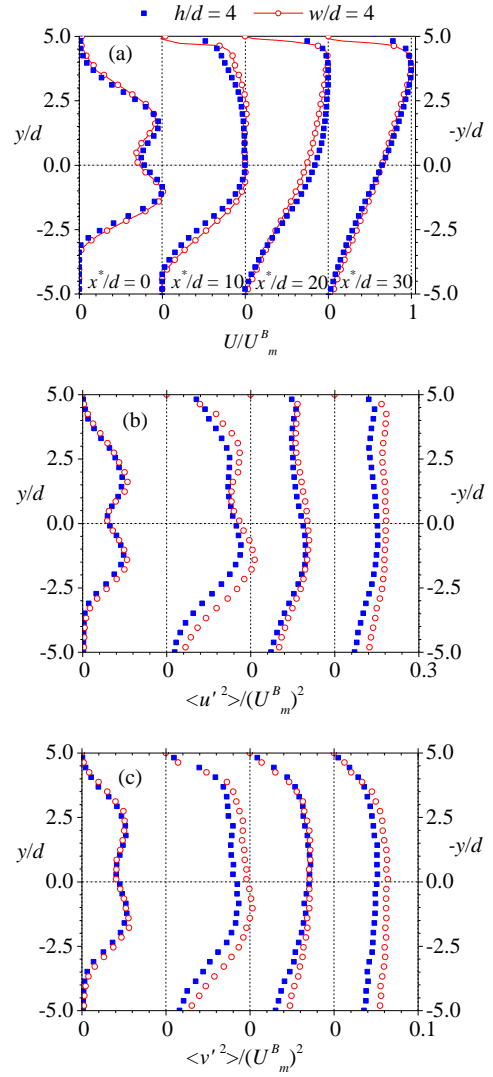
(Walker et al. 1995). The reduced transverse Reynolds normal stress and the concomitant increase in streamwise Reynolds normal stress indicate enhanced anisotropy near the boundary for each test case. The influence of the wall enhanced the Reynolds stresses more than their free surface counterparts.

Two-point correlations

Two-point correlation of the velocity fluctuations is used to investigate the effects of the offset ratio and boundary condition on the large scale structures along the center plane and near each boundary. The two-point auto-correlation function (R_{AB}) between any two arbitrary quantities $A (x, y)$ and $B (x, y)$ is evaluated as follows:

$$R_{AB}(x_{ref} + \Delta x, y_{ref} + \Delta y) = \frac{\langle A(x_{ref}, y_{ref}) B(x_{ref} + \Delta x, y_{ref} + \Delta y) \rangle}{\langle \sigma_A(x_{ref}, y_{ref}) \sigma_B(x_{ref} + \Delta x, y_{ref} + \Delta y) \rangle} \quad (2)$$
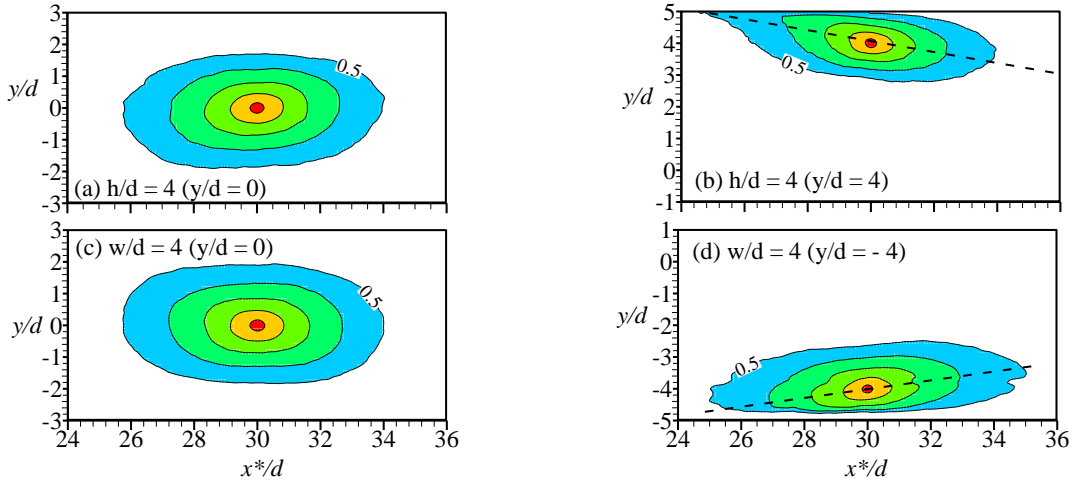
4

Figure 7. Iso-contours of the two-point autocorrelation of the streamwise velocity fluctuation, R_{uu} for $h/d = 4$ and $w/d = 4$.

where the point (x_{ref}, y_{ref}) denotes the reference location, Δx and Δy are the spatial separations between A and B in the streamwise and wall-normal directions, respectively, and σ_A and σ_B are the root-mean-square values of A and B at (x_{ref}, y_{ref}) and ($x_{ref} + \Delta x$, $y_{ref} + \Delta y$), respectively. The two-point correlation functions of the velocity fluctuations were calculated for each PIV realization and then ensemble-averaged point by point. Figure 7 shows iso-contours of the two-point autocorrelation of the streamwise velocity fluctuation, R_{uu} for $h/d = 4$ and $w/d = 4$ obtained at $x^*/d = 30$ on the center plane ($y/d = 0$) and near each boundary ($y/d = 4$ for $h/d = 4$ and $y/d = -4$ for $w/d = 4$). On the center plane, the contours of R_{uu} are aligned horizontally and elongated in the streamwise direction for each test condition. The elongation of the R_{uu} indicates streamwise alignment of vortices parallel to the center plane. Near each boundary, the R_{uu} contours show the presence of inclined structures, which are consistent with interacting hairpin vortices found

in turbulent boundary layers (Christensen and Adrian, 2001). The inclination angle is approximately 9° for structures obtained at $x^*/d \geq 25$. The iso-contours of the two-point correlation of the traverse velocity fluctuation, R_{vv} are shown Figure 8. The size of the R_{vv} contours are smaller and elongated in the transverse direction compared to the R_{uu} contours. As the boundary is approached, the effects of confinement reduced the size of the R_{vv} contours.

The size of the large scale structures can be estimated from the extents of the correlation functions. Following Volino et al. (2007), the streamwise extent of R_{uu} (L_{uux}) is determined as twice the distance from the self-correlation peak to the most downstream location on the 0.5 contour contour level while the transverse extent of R_{uu} (L_{uuy}) is defined as the transverse distance between points closest and farthest on the 0.5 contour level. The streamwise and transverse extents of R_{vv} (L_{vvx} and L_{vvy}) are defined as the distance between the closest and farthest point on the 0.5
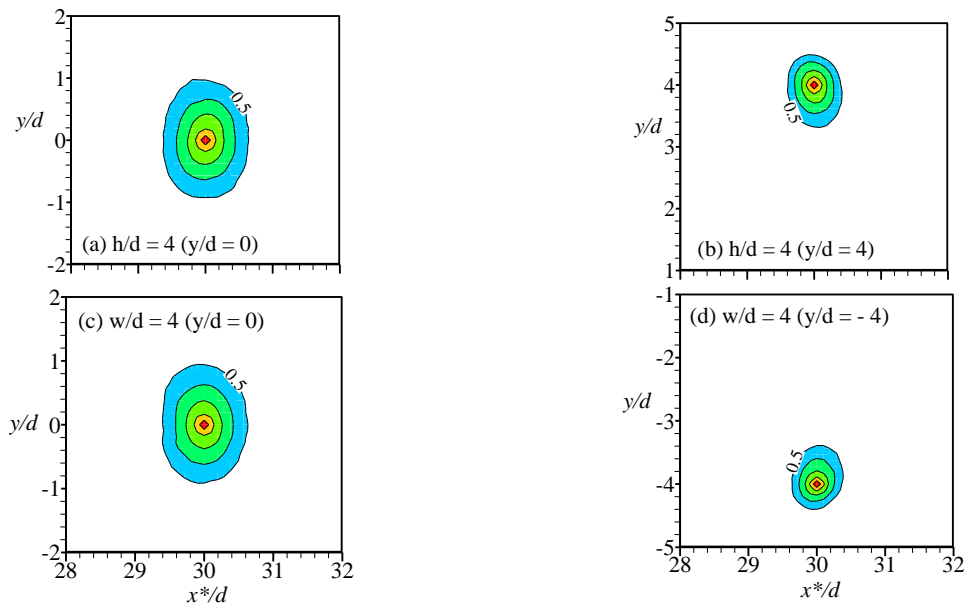

Figure 8. Iso-contours of the two-point autocorrelation of the transverse velocity fluctuation, R_{vv} for $h/d = 4$ and $w/d = 4$.
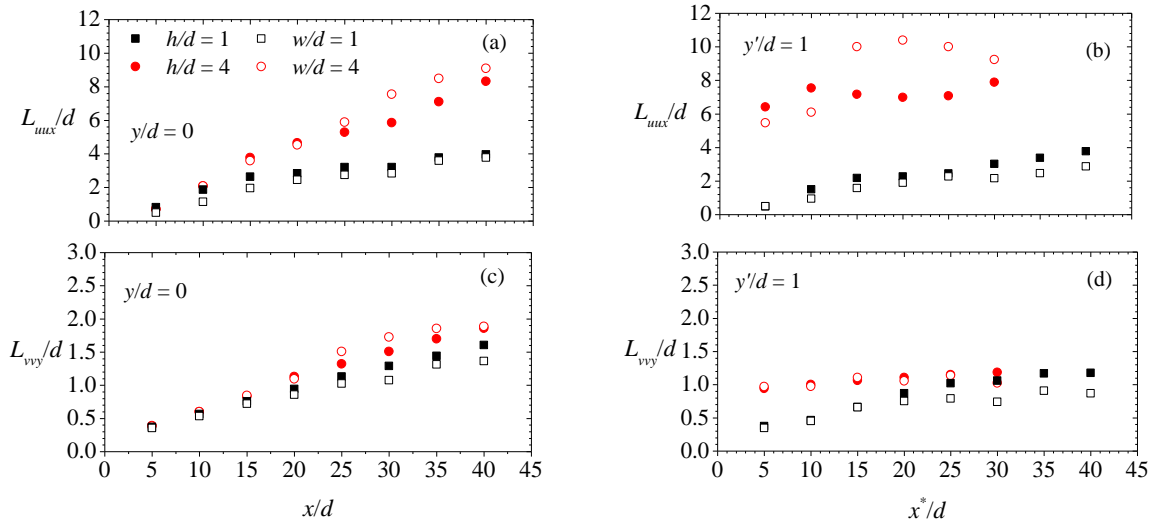
5

Figure 9. Distribution of extents, L_{uux} and L_{vvy} along center plane ($y/d = 0$) and near each boundary ($y'/d = 1$, where y' has an origin at the boundary).

contour level measured in the streamwise and transverse direction, respectively. The distributions of the largest extents of R_{uu} (L_{uux}) and R_{vv} (L_{vvy}) obtained along the center plane for the two extreme offset ratios are presented in Figure 9. The plots indicate that the size of the structures along the center plane is independent of confinement effects in the region, $x/d \leq 15$. Further downstream, the structures are reduced for the smaller offset ratios due to the reduction in entrainment rate and mixing as offset ratio decreased. Near the boundaries, the L_{uux} for $w/d = 4$ are longer over the solid wall than the free surface counterpart. In the far field ($x/d \geq 25$), the viscous effects near the wall reduced L_{vvy} compared to the values near the free surface.

CONCLUSION

A PIV technique was used to investigate the effects of offset ratio on the turbulence statistics of submerged twin jets interacting with a free surface and a solid wall. For both boundaries, the attachment length increased linearly with offset ratio. The jet-boundary interaction increased the combined point as offset ratio is reduced and the increase was larger over the solid wall than the free surface. The mean velocity decay rate reduced in the interaction region and effects of intercomponent energy transfer enhanced the anisotropy near each boundary. In the far field, the R_{uu} contours revealed the presence of inclined structures near each boundary. The viscous effects near the wall increased the streamwise extents of R_{uu} and decreased the transverse extents of R_{vv}.

ACKNOWLEDGEMENT

REFERENCES

Agelin-Chaab, M., and Tachie, M. F., 2011, "Characteristics of Turbulent Three-Dimensional Offset Jets." *Journal of Fluids Engineering*, Vol. 133, pp. 51203.

Essel, E. E., and Tachie, M.F., 2017, "Flow Characteristics of Submerged Twin Jets Interacting with Free Surface." *AIAA Journal*.

Christensen, K. T., and Adrian, R. J., 2001, "Statistical evidence of hairpin vortex packets in wall turbulence.", *Journal of Fluid Mechanics*, Vol. 431, pp. 433–443.

Harima, T., Fujita, S., and Osaka, H., 2001, "Mixing and Diffusion Processes of Twin Circular Free Jets with Various Nozzle Spacing." *Proceeding of World Conference on Experimental Heat Transfer, Fluid Mechanics, and Thermodynamics*, pp. 1017–1022.

Nozaki, T., 1983, "Reattachment Flow Issuing from a Finite Width Nozzle: Effects of Aspect Ratio of the Nozzle." *Bulletin of the JSME*, Vol. 26, pp. 1884–1890.

Perot, B., and Moin, P., 1995, "Shear-Free Turbulent Boundary Layers. Part 1 Physical Insights into near Wall Turbulence." *Journal of Fluid Mechanics*, Vol. 295, pp. 199–227.

Tay, G. F. K., Rahman, M. S., and Tachie, M. F., 2017, "Characteristics of a Square Jet Interacting with the Free Surface." *Physical Review Fluids*.

Todde, V., Spazzini, P. G., and Sandberg, M., 2009, "Experimental Analysis of Low-Reynolds Number Free Jets." *Experiments in Fluids*, Vol. 47, pp. 279–94.

Volino, R. J., Schultz, M. P., and Flack, K. A., 2007, "Turbulence Structure in Rough- and Smooth-Wall Boundary Layers." *Journal of Fluid Mechanics*, Vol. 592, pp. 263–93.

Walker, D. T., Chen, C.-Y. and Willmarth, W. W., 1995, "Turbulent Structure in Free-Surface Jet Flows." *Journal of Fluid Mechanics*, Vol. 291, pp. 223–261.

Wang, X. K., and Tan, S. K., 2007, "Experimental Investigation of the Interaction between a Plane Wall Jet and a Parallel Offset Jet." *Experiments in Fluids*, Vol. 42, pp. 551–562.